Slug flow modeling

During the hydrocarbon transport in subsea pipelines, gas and oil flow concurrently as gas gradually liberates out upon temperature and pressure drops. In such conditions, slug flow is the dominant flow regime which occurs over a wide range of gas and liquid flow rates. Therefore, it is imperative to have a modeling tool to predict paraffin deposit characteristics under two-phase gas-oil slug flow regime. For this purpose, pressure and temperature should be predicted and included in the wax deposition modeling. Due to the slug flow's intermittent and unsteady nature, a mechanistic model was required to develop to account for the transient behavior of the flow for pressure drop and heat transfer calculations.

• Hydrodynamic Properties

Accurate heat transfer and pressure drop calculations are greatly dependent on correct hydrodynamic properties. We employed different models and developed a code to predict various slug flow hydrodynamic properties. Taitel and Barnea Slug Model [1] was primarily used with full film profile calculation. The following ODE was solved numerically using RKF45 adaptive ODE solving method.

$$\frac{dh_F}{dz} = \frac{\frac{\tau_F S_F}{A_F} - \frac{\tau_G S_G}{A_G} - \tau_I S_I \left(\frac{1}{A_F} + \frac{1}{A_G}\right) + (\rho_L - \rho_G) g sin\theta}{(\rho_L - \rho_G) g cos\theta - \rho_L v_F \frac{(v_{TB} - v_{LLS}) H_{LLS}}{H_{LTB}^2} \frac{dH_{LTB}}{dh_F} - \rho_G v_G \frac{(v_{TB} - v_{GLS})(1 - H_{LLS})}{(1 - H_{LTB})^2} \frac{dH_{LTB}}{dh_F}} \quad (1)$$

where τ_F, τ_G and τ_I are shear stress terms and are calculated as:

$$\tau_F = f_F \frac{\rho_L |v_{LTB}| v_{LTB}}{2} \quad (2)$$

$$\tau_G = f_G \frac{\rho_G |v_{GTB}| v_{GTB}}{2} \quad (3)$$

$$\tau_I = f_I \frac{\rho_G |v_{GTB} - v_{LTB}| (v_{GTB} - v_{LTB})}{2} \quad (4)$$

Where v_{GTB} and v_{LTB} are gas and liquid actual velocities in the film region. Also, f_F, f_I and f_G are friction factor terms which are calculated from Fanning friction factor formula:

$$\frac{1}{\sqrt{f}} = -4 \log\left(\frac{\epsilon}{3.7d} + \frac{1.256}{Re\sqrt{f}}\right) \quad (5)$$

In the calculations, several geometrical parameters of stratified flow are needed, some of which include: liquid (S_L), gas (S_G) and interface (S_I) in the film region.

$$\tilde{S}_F = \pi - \cos^{-1}\left(2\tilde{h}_L - 1\right) \tag{6}$$

$$\tilde{S}_I = \sqrt{1 - \left(2\tilde{h}_L - 1\right)^2} \tag{7}$$

$$\tilde{S}_G = \cos^{-1}(2\tilde{h}_L - 1) \tag{8}$$

$$S_F = \tilde{S}_F d^2,\ S_I = \tilde{S}_I d^2,\ S_G = \tilde{S}_G d^2 \tag{9}$$

And similarly, the surface areas of each phase is represented as:

$$\tilde{A}_L = 0.25\left[\pi - \cos^{-1}\left(2\tilde{h}_L - 1\right) + \left(2\widetilde{h_L} - 1\right)\sqrt{1 - \left(2\tilde{h}_L - 1\right)^2}\right] \tag{10}$$

$$\tilde{A}_G = 0.25\left[\cos^{-1}\left(2\tilde{h}_L - 1\right) - \left(2\tilde{h}_L\ - 1\right)\sqrt{1 - \left(2\tilde{h}_L - 1\right)^2}\right] \tag{11}$$

$$A_L = \tilde{A}_L d^2,\ A_G = \tilde{A}_G d^2 \tag{12}$$

And hydraulic diameters can be calculated as

$$d_L = 4\frac{A_L}{S_L} \tag{13}$$

$$d_G = \frac{4A_G}{S_G + S_I} \tag{14}$$

Another important hydrodynamic parameter which is needed in our calculation is the wetted angle.

If $\theta < \pi$

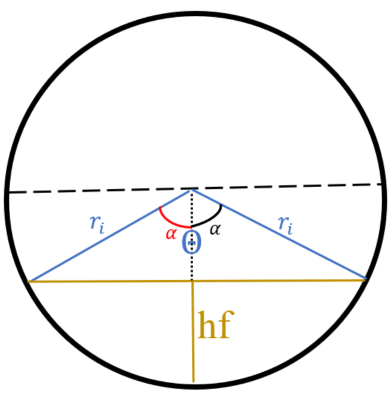

Figure 1: Wetted angle where $h_f\ < r_i$

$$\alpha = \arccos(\frac{r_i - h_f}{r_i}) \tag{15}$$

$$\theta = 2 * \arccos(\frac{r_i - h_f}{r_i}) \tag{16}$$

If $\theta > \pi$

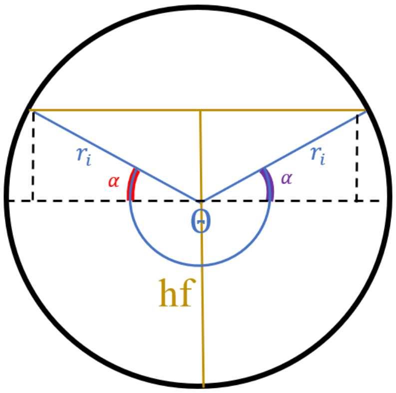

Figure 2: Wetted angle where $h_f > r_i$

$$\theta = 2 * \arccos(\frac{r_i - h_f}{r_i}) \tag{17}$$

$$\theta = \pi + 2 * \arcsin(\frac{h_f - r_i}{r_i}) \tag{18}$$

It is in high importance to distinguish the difference between h_F and H_{LTB}. h_F is the liquid height in [m] and H_{LTB} is the liquid holdup in the film region. From Eq. (1), h_F profile is calculated and the following relation should be used to convert it to H_{LTB} profile.

$$H_{LTB} = \frac{1}{\pi}\left[\pi - \cos^{-1}\left(2\tilde{h}_L - 1\right) + \left(2\tilde{h}_L - 1\right) * \sqrt{1 - \left(2\tilde{h}_L - 1\right)^2}\right] \tag{19}$$

And consequently,

$$\frac{dH_{LTB}}{dh_F} = \frac{4}{\pi d}\sqrt{1 - \left(2\tilde{h}_L - 1\right)^2} \tag{20}$$

Another important parameter is liquid holdup in slug region (H_{LLS}). We have used different approaches and found out that most equations overestimate the value of H_{LLS}. Zhang et. al. [2] model (shown below) was the best candidate and has been used in our study. In their model, intermittent hydrodynamic properties of slug-flow were taken into account through solving a series of continuity and momentum equations.

$$H_{LLS} = \frac{1}{1 + \frac{Zh_{sm}}{3.16 * \left[(\rho_L - \rho_g) g \sigma\right]^{0.5}}} \tag{21}$$

Where Zh_{sm} is Zhang et al. shear stress and mixing term

$$Zh_{sm} = \frac{1}{C_B}\left[\frac{f_s}{2}\rho_s v_m^2 + \frac{d}{4}\frac{\left(\rho_L \bar{H}_{LTB}(v_{Tb} - \bar{v}_{LTB})(v_M - \bar{v}_{LTB})\right)}{L_s}\right] \tag{22}$$

In Eq. (22), subscript "s" is associated to the slug body. In the slug section, the properties are calculated from weighted average of gas and liquid properties based on H_{LLS}. In addition, $\bar{H}_{LTB}$ and $\bar{v}_{LTB}$ are average liquid holdup and average liquid velocity in the film region, respectively. Since the full film profile calculation is included in our study, the average values for $\bar{H}_{LTB}$ and $\bar{v}_{LTB}$ should be used as follows:

$$\bar{H}_{LTB} = \frac{\int_{L_S}^{L_U} H_{LTB_z} dz}{L_f} \tag{23}$$

where v_{LTB} is calculated from

$$\bar{v}_{LTB} = v_{Tb} - \bar{v}_F \tag{24}$$

v_F is the relative velocity referenced to the translational velocity and it is calculated as:

$$\bar{v}_F = (v_{Tb} - v_{LLS}) * \frac{H_{LLS}}{\bar{H}_{LTB}} \tag{25}$$

v_{Tb} and v_{LLS} are transitional velocity and liquid phase's velocity in the slug region, respectively. They can be calculated from the following relations:

$$v_{Tb} = C_0 v_M + 0.54 * \sqrt{gd} \tag{26}$$

$$v_{LLS} = \frac{v_M - v_{GLS} * (1 - H_{LLS})}{H_{LLS}} \tag{27}$$

and v_M is the mixture velocity in the slug section

$$v_M = v_{SL} + v_{SG} \tag{28}$$

Finally, the inclination dimensionless coefficient (C_B) can be calculated as:

$$C_B = \frac{2.5 - |sin\theta|}{2} \tag{29}$$

Please note that in Eq. (21), H_{LLS} is in implicit form and needs to be solved iteratively. The iteration stops when the following criteria is satisfied.

$$\left|\bar{H}_{LTB_{New}} - \bar{H}_{LTB_{Pre}}\right| < \epsilon_1 \tag{30}$$

Where $\bar{H}_{LTB_{New}}$ and $\bar{H}_{LTB_{Pre}}$ are the corresponding average film liquid holdups from newly calculated H_{LLS} and from the previous H_{LLS}.

It is advised to use Gregory et al. [3] correlation (shown below) for the initial value of H_{LLS}.

$$H_{LLS} = \frac{1}{1 + \left(\frac{v_M}{8.66}\right)^{1.39}} \tag{31}$$

The rest of velocity terms are:

$$v_G = (v_{Tb} - v_{GLS}) * \frac{1 - H_{LLS}}{1 - H_{LTB}} \tag{32}$$

$$v_{GTB} = v_{Tb} - v_G \tag{33}$$

$$v_{GLS} = C_0 v_M \tag{34}$$

Another parameter, which should be estimated using closure relationship, is either slug length or slug frequency. In our study, we have used $L_s = 30D$ which is the most acceptable approximation for slug length. Other velocity terms are calculated from the following relations.

Now, all required parameters are available and Eq. (1) can be solved using proper boundary conditions.

$$\text{At } z = 0,\ H_{LTB_0} = H_{LLS} \text{ or } h_{F_0} = h_{LLS} \tag{35}$$

However, after double-checking the convergence for the variety of gas and liquid superficial velocities, it was found that Eq. (35) does not always work because h_{LLS} is not always less than critical liquid height (h_C). So, we needed to introduce a new initial condition (shown below) for solving the ODE.

$$\text{At Z=0} \begin{cases} \text{If } h_{LLS} < h_C \text{ then } h_{F_0} = h_{LLS} & (36) \\ \text{If } h_{LLS} > h_C \text{ then } h_{F_0} = h_C & (37) \end{cases}$$

h_C can be calculated from the following relation.

$$(\rho_L - \rho_G)gcos\theta - \rho_L v_F \frac{(v_{TB} - v_{LLS})H_{LLS}}{H_{LTB}^2}\frac{dH_{LTB}}{dh_F} - \rho_G v_G \frac{(v_{TB} - v_{GLS})(1 - H_{LLS})}{(1 - H_{LTB})^2}\frac{dH_{LTB}}{dh_F} \tag{38}$$

where H_{LTB_C} is calculated from Eq. (19) when h_f is replaced by h_C

By knowing the above boundary condition, the ODE can be solved for $Z = [0, L_f]$. However, film length (L_f) is another parameter which is unknown and is expected to be calculated as an important hydrodynamic property from our modeling. For any value of L_f, we used the following equation for liquid mass flow rate [4] ($W_{L,Cal}$) and compared it to the input mass flow rate ($W_{L,Input}$). Then, L_f was properly adjusted till $\epsilon_{L,Mass}$ (shown below) is smaller than a certain tolerance.

$$W_{L,Cal} = \left(\rho_L L_s A_p H_{LLS} + \int_0^{L_f} \rho_L A_p H_{LTB} dL \right) \frac{1}{T_U} - x \tag{39}$$

$$\left| W_{L,Cal} - W_{L,Input} \right| < \epsilon_2 \tag{40}$$

Where T_U is the unit length time and is calculated as,

$$T_U = \frac{V_{TB}}{L_u} \tag{41}$$

And x is picking/shedding rate and is expressed as:

$$x = (v_{Tb} - v_{LLS}) \rho_L A_P H_{LLS} \tag{42}$$

Newton Raphson root finding method was used to find the correct L_f that results in minimum error in Eq.*40*.

The presented theory for the calculation of hydrodynamic properties does not include the temperature parameter (isothermal process), even though the slug's temperature constantly changes as it moves in the pipe. This is very important because any change in the temperature results in different fluid properties. In our study, we introduced a methodology to include temperature effect in hydrodynamic property calculation. As illustrated in Figure 3, initially, the hydrodynamic properties are calculated using the initial slug unit temperature ($\bar{T}_{Initial}$) at $t = 0$. Next, the heat transfer modeling is called to estimate the temperature distribution in the slug. Then the average unit slug's temperature ($\bar{T}_{Slug}$) during $\Delta t = T_u$ is calculated and used to update the hydrodynamic properties. If the newly calculated hydrodynamic properties are similar to the previous iteration, the process will stop and the properties are reported. If enough similarity was not achieved, this process continues.

In the lab-scale experiments, such update might not have significant effect however, in the field case where the pipeline is several miles long, the mentioned updating process should be included. In Figure 4, the gas-core temperature of two cases where isothermal and non-isothermal conditions are assumed is shown. In the non-isothermal case, the proposed methodology (as shown in Figure 3) is used while, in the isothermal case, only initial slug's temperature was used to calculate the hydrodynamic properties. Notably, the results show more difference with time.

97
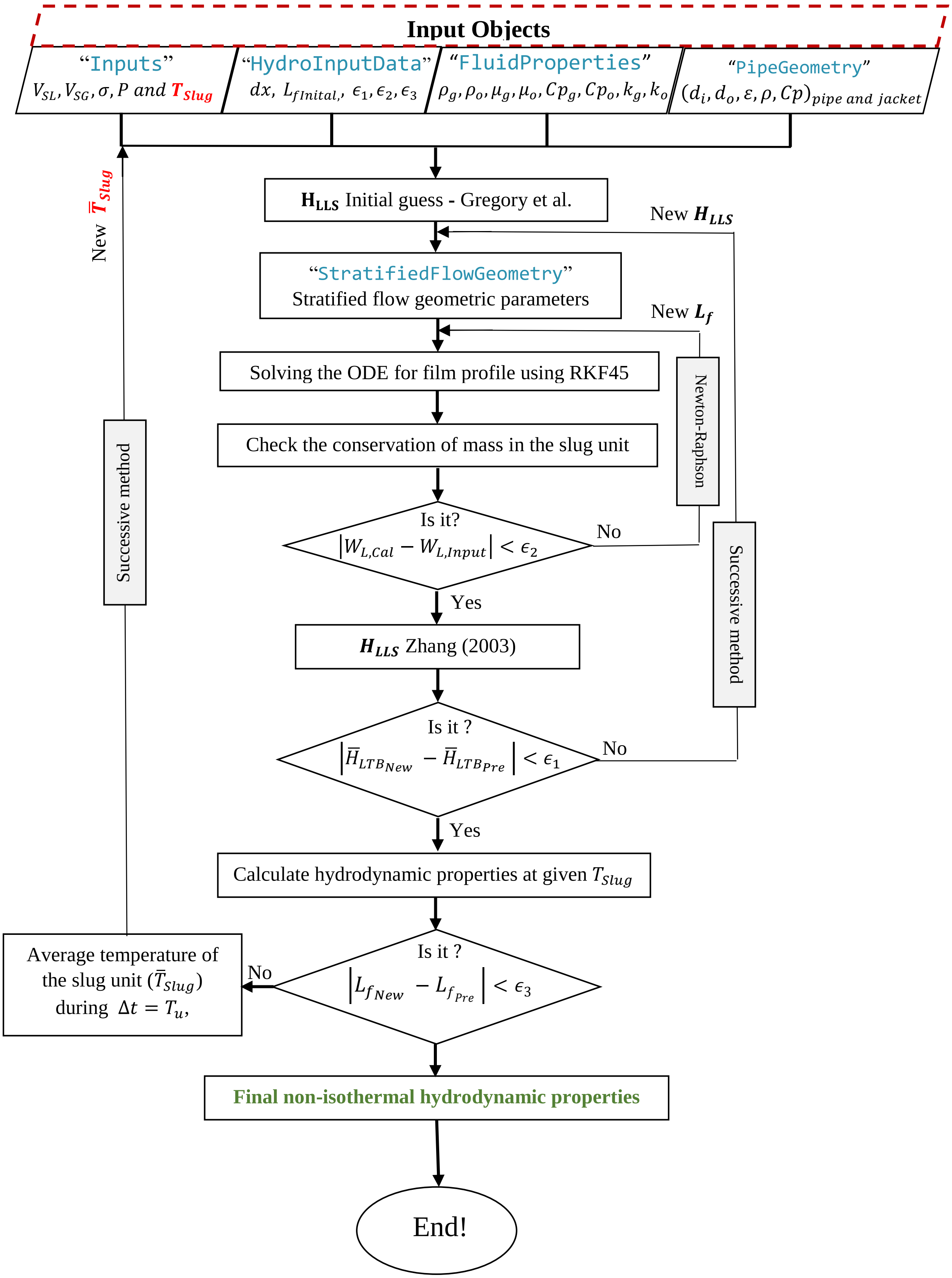

98
Figure 3: Flow chart of the developed hydrodynamic modeling

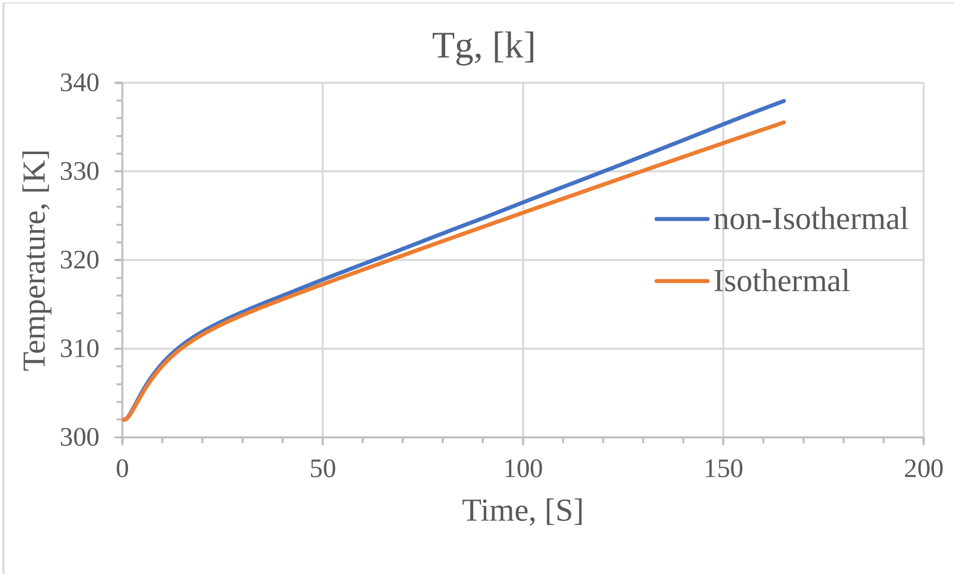

Figure 4: Average gas-core temperature for q=12000[$\frac{w}{m^2}$] for two cases where isothermal and non-isothermal assumptions are made for the calculation of hydrodynamic properties of Garden Banks oil type and $v_{SL} = 1\frac{ft}{s}$ & $v_{SG} = 4\frac{ft}{s}$

In the following section, a thorough sensitivity analysis of hydrodynamic properties has been conducted and the results are shown. In the following schematic, the full film profile in the stratified flow section is shown with all parameters which will be calculated by our simulation. Non-uniform discretization has been used for liquid height calculation.

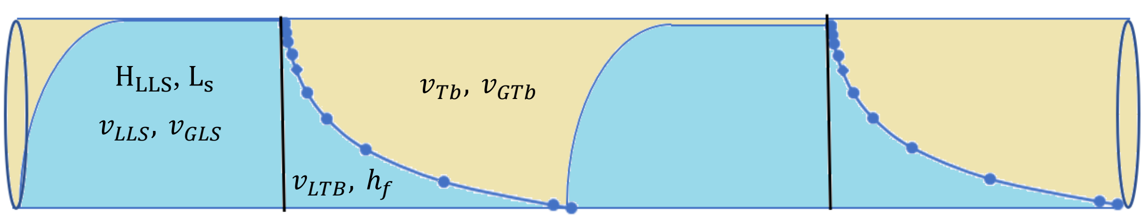

Figure 5: The schematic of slug flow with full film profile calculation and the associated parameters

In the following graphs, different hydrodynamic properties are calculated and plotted for different superficial gas and liquid velocities. In Figure 6, the final film lengths versus different v_{SL} and v_{SG} are calculated and plotted. Expectedly, L_f is shorter when liquid superficial velocity (v_{SL}) increases.

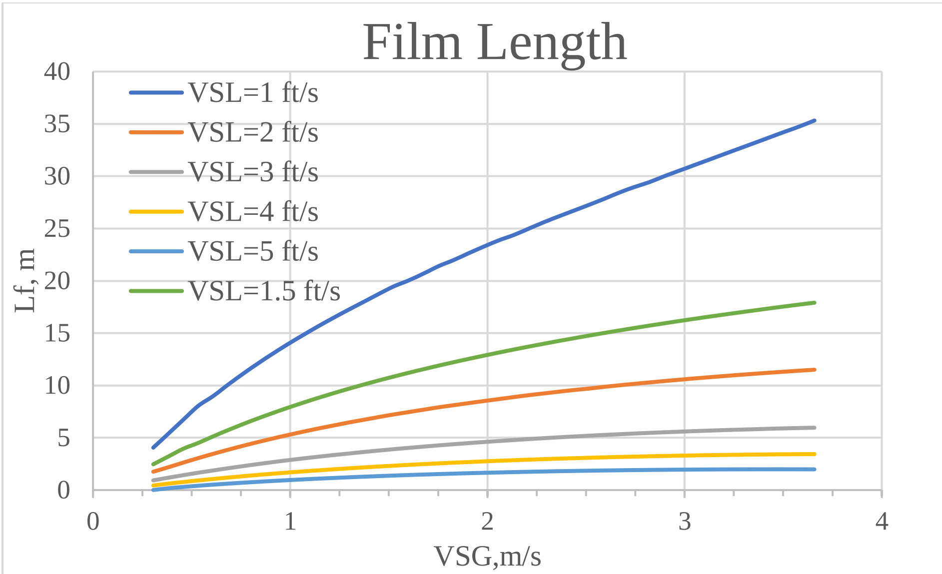

Figure 6: Final film length for different liquid and gas superficial velocities at $P = 350\ Psig$ and $T = 29°C$ using thermophysical and pipe properties of Rittirong (2014)

In the next graph, liquid holdup values in slug section (H_{LLS}) have been calculated and plotted. H_{LLS} decrease as v_{SL} increases for a certain v_{SG}. Similarly, H_{LLS} decreases as v_{SG} increases for a certain v_{SL}. This behavior is similar to results shown by Kora et al. (2011). For our next parameter, the average liquid holdup in the film region is calculated by integrating the full film profile over the film length. The trapezoidal method was used for integration. In below figure is the analysis of average liquid holdup in the film region.

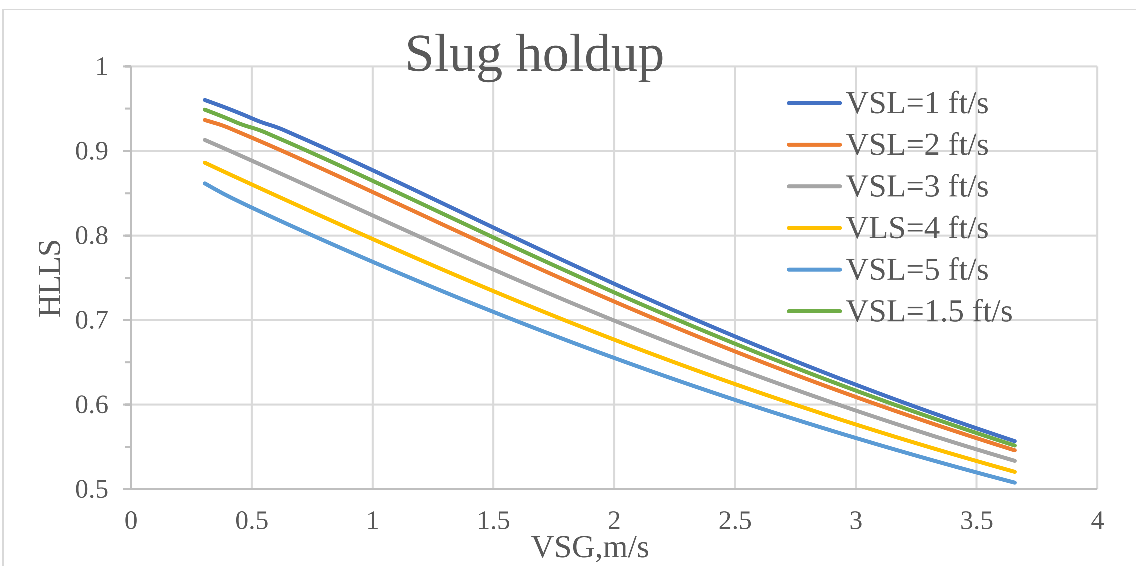

Figure 7:Slug holdup for different superficial liquid and gas velocities at P=350 Psig and T=29°C using thermophysical and pipe properties of Rittirong (2014)

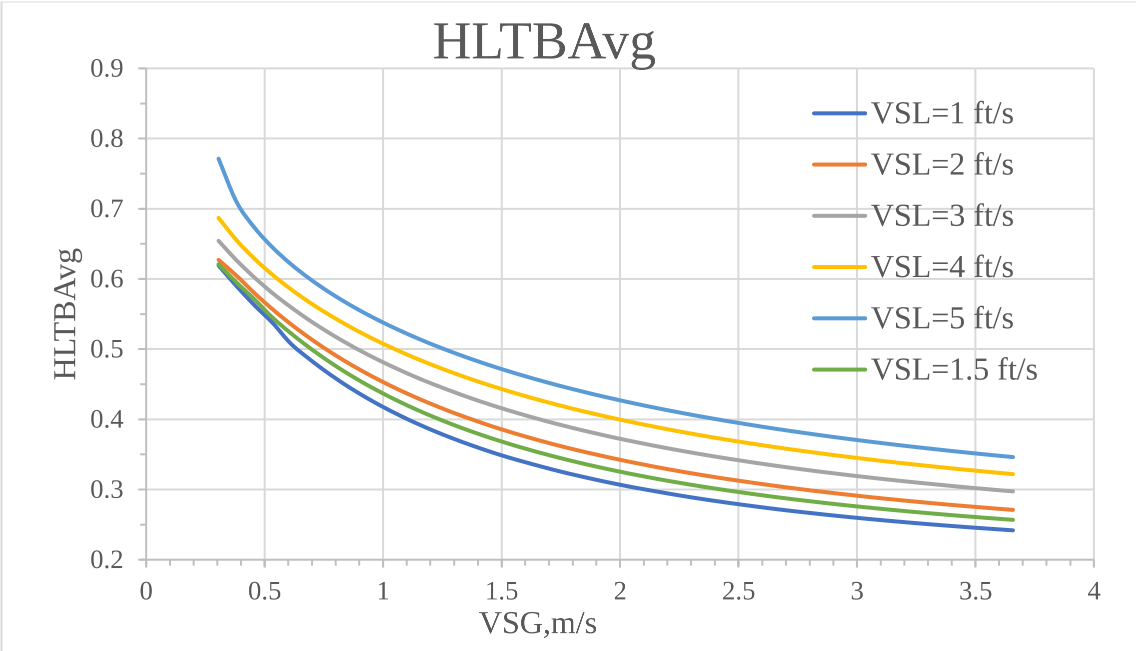

Figure 8: Average film holdup over L_f for different liquid and gas superficial velocities at $P = 350\ Psig$ and $T = 29°C$ using thermophysical and pipe properties of Rittirong (2014)

For full film profile calculation, Eq. (1) is solved using RKF45 adaptive method. In the following figure, full film profiles are plotted for 4 different cases.

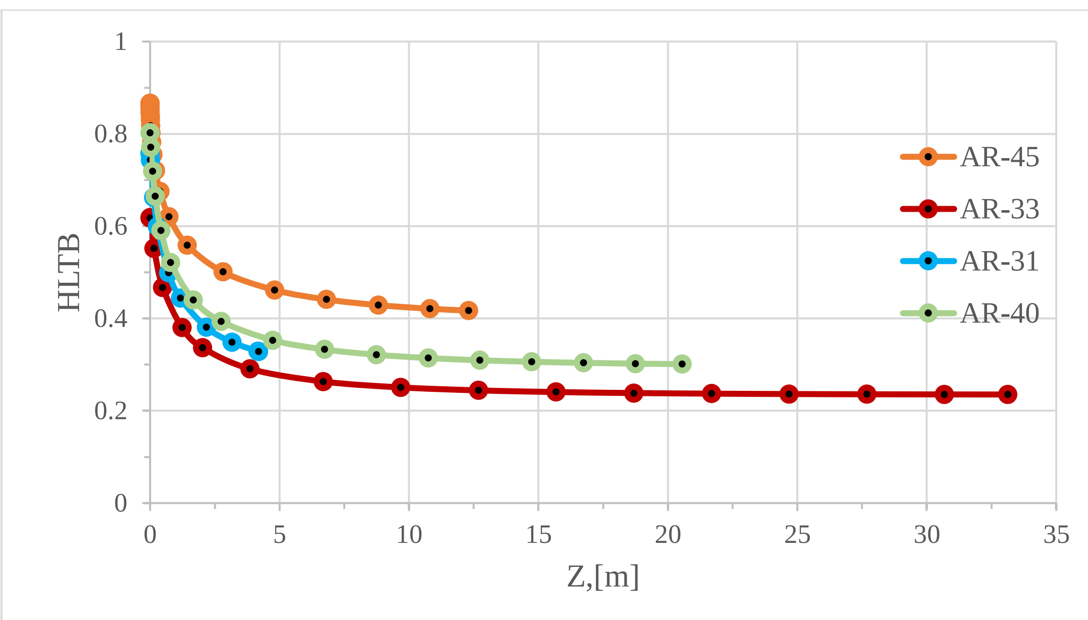

Figure 9: Full film profile curves of four cases of Rittirong (2014). Z is the axial direction from $Z = 0\ to\ Z = L_f$. The analyzed test are AR-33 ($v_{SL} = 1\frac{ft}{s}, v_{SG} = 10\frac{ft}{s}$), AR-45 ($v_{SL} = 1\frac{ft}{s}, v_{SG} = 2\frac{ft}{s}$), AR-31 ($v_{SL} = 3\frac{ft}{s}, v_{SG} = 5\frac{ft}{s}$) and, AR-40 ($v_{SL} = 1\frac{ft}{s}, v_{SG} = 5\frac{ft}{s}$)

• Pressure Drop

Pressure drop calculation is a vital component of the wax deposition modeling. Along the pipe, when pressure decreases, the thermophysical properties of gas change considerably. Therefore, pressure should be estimated in every axial location in combination with temperature. In our software, we use the Taitel and Barnea model [1] to predict the average pressure drop within a slug unit. In this model, the previously calculated hydrodynamic properties are used in the following pressure drop equation.

$$\Delta P_U = \frac{\tau_S \pi d}{A_p} L_s + \frac{\tau_F S_F}{A_p} L_f + \frac{(\tau_G S_G)}{A_p} L_f \tag{43}$$

The first terms represent the pressure drop associated with liquid slug and the other two expressions are pressure drops in the film zone. The following graph shows the pressure gradient term for different gas and liquid superficial velocities. Pressure gradient increases with the increase of v_{SL}. In addition, when the gas phase flowrate increases, $\frac{dP}{dL}$ term decreases as expected.

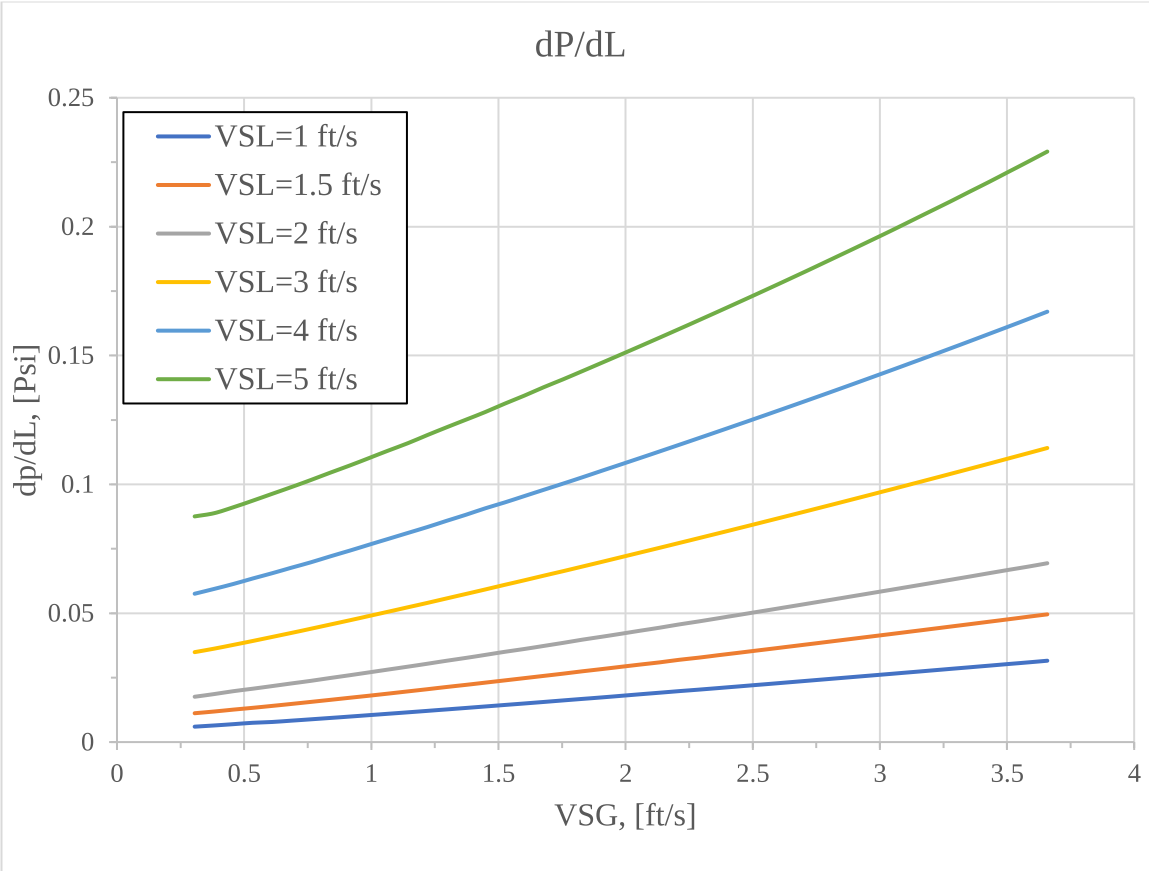

Figure 10: Pressure gradient curves for different gas and liquid superficial velocities at $T = 29°C$ and $p_{intial} = 350\ Psig$ using thermophysical and pipe properties of Rittirong (2014)

From Figure 10, it can be seen that pressure drop in long subsea pipelines can be significant and it is necessary to be calculated and included in the calculations. After knowing the hydrodynamic properties and pressure gradient, heat transfer modeling can be developed.

• Heat Transfer

Temperature arguably is the only factor that controls the wax precipitation. Therefore, it is imperative to have a reliable heat transfer modeling to predict liquid and gas temperatures along with pipe's wall temperature accurately. Slug flow is a complex flow regime that possesses an intermittent and unsteady nature. For example, at a certain axial location in the pipe, the wall is periodically exposed to a stratified flow pattern where gas and liquid flow on the top of each other and to a series of fast-moving liquid slugs that bridges the pipe. In addition, differences in thermophysical properties and velocities of each phase make it more difficult to predict the temperature. In our study, we have developed a transient slug flow heat transfer model using a mixed Eulerian/Lagrangian approach.

In this section, theoretical framework of the developed modeling is presented. The basic of our modeling approach is to account for all the possible energies that either enter or leave a control volume of the fluid/wall/deposit and then to calculate the temperature increase/decrease based on the associated properties. In other word, we used the concept of energy balance as a basis of our heat transfer modeling. Initially, Niu and Dukler [5] introduced this approach only for constant heat flux in water/air system. However, in our study, we further extended this approach for wax deposition case in counter-current pipe-in-pipe flow with complete hydrodynamic model. In our modeling the direction of heat is considered in all three dimensions (x, r and θ). In the following graph, the incoming and outcoming energies to a control volume of the pipe are shown.

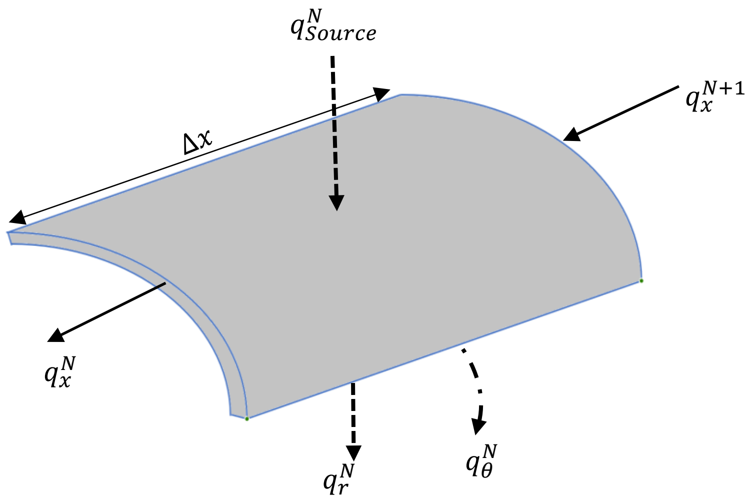

The pipe's wall is further discretized in radial and in circumferential directions as follows:

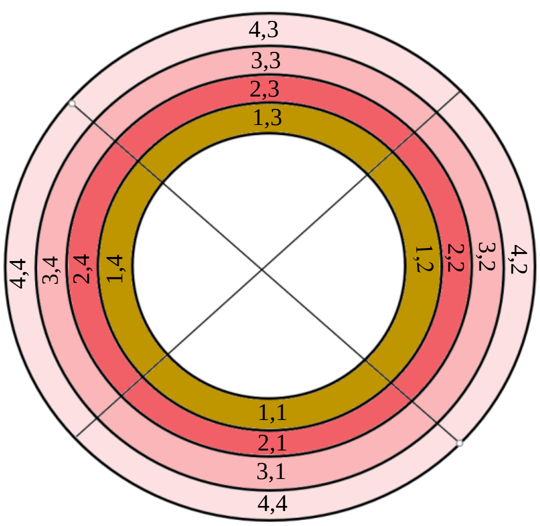

Figure 11: A snapshot of the front of the pipe with deposited wax with radial and circumferential discretization

Based on the discretized segments in Figure 11, the mathematical formulas are derived. Although, the properties of pipe's segments are constant, wax deposit's characteristics change circumferentially and axially. Such circumferential variance exists because different sections of the wax deposit is periodically exposed to different fluids with varying temperatures. In the following section, a new heat transfer model is derived when wax is present.

The heat transfer modeling requires the hydrodynamic properties of the slug flow. However, hydrodynamic properties are calculated based on constant fluid properties and inner pipe radius. There is an inconsistency because temperature changes in nearly all directions which result in changes in properties. In addition, the effective pipe's radius varies axially and circumferentially. All these changes cannot be considered in the hydrodynamic model. Therefore, we came up with an approach to make our model consistent.

1- The inlet temperature and the average effective ID of the first axial interval is considered, and hydrodynamic properties are calculated.
2- Based on the calculated hydrodynamic properties, heat transfer model will be executed, and the temperature distribution will be determined for a calculated L_u
3- Average bulk temperature over a slug unit length is then calculated.
4- From the previously calculated bulk temperature, average fluid properties are calculated. In addition, average ID over the slug unit length is calculated.
5- The average fluid properties and ID are used to recalculate the hydrodynamic properties.
6- The newly calculated L_u is then compared to the precious L_u. If the difference is small, then we accept it otherwise step 2 to 5 will be repeated

Before start writing the detailed formulas, please be aware that the thicknesses in inner wall segments are not the same. So the $A_{p_{ef}}[x] = \frac{\pi}{4}\left(r_i - w_{BotDepo}[x]\right)^2 + \frac{\pi}{4}\left(r_i - w_{UpDepo}[x]\right)^2 + \frac{\pi}{2}\left(r_i - w_{SideDepo}[x]\right)^2$

Ring 9 derivation

- Energy from the source (out)

$$E_s[x][4][3](J) = q[x]\left(\frac{J}{\mathrm{s.m}^2}\right) * A_{out}[4](m^2) * \Delta t(s)$$

$$A_{out}[4] = \left(\frac{\pi r_0}{2} * \Delta x\right)$$

- Energy from radial direction (in this problem, from the bottom to the top)

$$E_r[x][4][3](J) = A_{In}[4](m^2) * k_w\left(\frac{J}{m.{}^\circ K.s}\right) * \frac{\mathrm{T}[x][3][3] - \mathrm{T}[x][4][3]}{\frac{\mathrm{w_p}}{3}}(^\circ\mathrm{K}) * \Delta\mathrm{t}(s)$$

$$A_{In}[4] = \left(\frac{\pi}{2}\left(r_0 - \frac{w}{3}\right) * \Delta x\right)$$

- Energy in axial direction

$$E_x[x][4][3](J) = E_{x_{in}} - E_{x_{out}}$$

$$E_{x_{out}} = -A_x[4](m^2) * k_w\left(\frac{J}{m.{}^\circ K.s}\right) * \frac{T[x+1][4][3] - T[x][4][3]}{\Delta x}\left(\frac{^\circ K}{m}\right) * \Delta t(s)$$

$$E_{x_{in}} = -A_x[4](m^2) * k_w\left(\frac{J}{m.{}^\circ K.s}\right) * \frac{T[x][4][3] - T[x-1][4][3]}{\Delta x}\left(\frac{^\circ K}{m}\right) * \Delta t(s)$$

$$E_x[x][4][3](J) = A_x[4](m^2) * k_w\left(\frac{J}{m.°K.s}\right) * \frac{T[x+1][4][3] - 2 * T[x][4][3] + T[x-1][4][3]}{\Delta x}\left(\frac{°K}{m}\right) * \Delta t(s)$$

$$A_x[4](m^2) = \left(\frac{\pi}{2} * \left(r_0 - \frac{w}{6}\right) * \frac{w}{3}\right)$$

- energy stored in angular direction

$$E_\theta[x][4][3](J) = E_{\theta_{in}} - E_{\theta_{out}}$$

$$E_{\theta_{in}} = -A_\theta[4](m^2) * k_w\left(\frac{J}{m.°K.s}\right) * \frac{T[x][4][2] - T[x][4][3]}{\Delta x_\theta[4]}\left(\frac{°K}{m}\right) * \Delta t(s)$$

$$E_\theta[x][4][3](J) = -A_\theta[4](m^2) * k_w\left(\frac{J}{m.°K.s}\right) * \frac{T[x][4][3] - T[x][4][4]}{\Delta x_\theta[4]}\left(\frac{°K}{m}\right) * \Delta t(s)$$

Since $T[x][4][4] = T[x][4][2]$

$$E_\theta[x][4][3](J) = A_\theta[4](m^2) * k_w\left(\frac{J}{m.°K.s}\right) * \frac{T[x][4][4] - 2 * T[x][4][3] + T[x][4][2]}{\Delta x_\theta[4]}\left(\frac{°K}{m}\right) * \Delta t(s)$$

$$A_\theta[4](m^2) = \frac{w}{3} * \Delta x, \qquad \Delta x_\theta[4](m) = \frac{\pi}{2} * \left(r_0 - \frac{w}{6}\right)$$

Ring 9 final,

$$E_s[x][4][3] = q[x] * A_{out}[4] * \Delta t$$

$$E_r[x][4][3] = A_{In}[4] * k_w * \frac{\mathrm{T}[x][3][3] - \mathrm{T}[x][4][3]}{\frac{\mathrm{w}}{3}} * \Delta \mathrm{t}$$

$$E_x[x][4][3](J) = A_x[4] * k_w * \frac{T[x+1][4][3] - 2 * T[x][4][3] + T[x-1][4][3]}{\Delta x} * \Delta t$$

$$E_\theta[x][4][3](J) = A_\theta[4] * k_w * \frac{T[x][4][4] - 2 * T[x][4][3] + T[x][4][2]}{\Delta x_\theta[4]} * \Delta t$$

Ring 8 final,

$$E_s[x][4][2] = q[x] * A_{out}[4] * \Delta t$$

$$E_r[x][4][2] = A_{In}[4] * k_w * \frac{\mathrm{T}[x][3][2] - \mathrm{T}[x][4][2]}{\frac{\mathrm{w}}{3}} * \Delta \mathrm{t}$$

$$E_x[x][4][2](J) = A_x[4] * k_w * \frac{T[x+1][4][2] - 2 * T[x][4][2] + T[x-1][4][2]}{\Delta x} * \Delta t$$

$$E_\theta[x][4][2](J) = A_\theta[4] * k_w * \frac{T[x][4][3] - 2 * T[x][4][2] + T[x][4][1]}{\Delta x_\theta[4]} * \Delta t$$

Ring 7 final,

$$E_s[x][4][1] = q[x] * A_{out}[4] * \Delta t$$

$$E_r[x][4][1] = A_{In}[4] * k_w * \frac{\mathrm{T}[x][3][1] - \mathrm{T}[x][4][1]}{\frac{\mathrm{w}}{3}} * \Delta \mathrm{t}$$

$$E_x[x][4][1](J) = A_x[4] * k_w * \frac{T[x+1][4][1] - 2 * T[x][4][1] + T[x-1][4][1]}{\Delta x} * \Delta t$$

$$E_\theta[x][4][1](J) = A_\theta[4] * k_w * \frac{T[x][4][2] - 2 * T[x][4][1] + T[x][4][4]}{\Delta x_\theta[4]} * \Delta t$$

Ring 6 final,

$$E_s[x][3][3] = \frac{A_{out}[3] * k_w * (\mathrm{T}[x][4][3] - \mathrm{T}[x][3][3]) * \Delta t}{\frac{w}{3}}$$

$$E_r[x][3][3] = A_{In}[3] * k_w * \frac{\mathrm{T}[x][2][3] - \mathrm{T}[x][3][3]}{\frac{\mathrm{w}}{3}} * \Delta \mathrm{t}$$

$$E_x[x][3][3](J) = A_x[3] * k_w * \frac{T[x+1][3][3] - 2 * T[x][3][3] + T[x-1][3][3]}{\Delta x} * \Delta t(s)$$

$$E_\theta[x][3][3](J) = A_\theta[3] * k_w * \frac{T[x][3][2] - 2 * T[x][3][3] + T[x][3][4]}{\Delta x_\theta[3]} * \Delta t(s)$$

$$A_{out}[3] = \left(\frac{\pi}{2}\left(r_0 - \frac{w}{3}\right) * \Delta x\right), A_{In}[3] = \left(\frac{\pi}{2}\left(r_0 - 2\frac{w}{3}\right) * \Delta x\right), A_x[3] = \left(\frac{\pi}{2} * \left(r_0 - \frac{w}{3} - \frac{w}{6}\right) * \frac{w}{3}\right),$$

$$A_\theta[3] = \left(\frac{w}{3} * \Delta x\right), \Delta x_\theta[3] = \frac{\pi}{2} * \left(r_0 - \frac{w}{3} - \frac{w}{6}\right)$$

Ring 5 final,

$$E_s[x][3][2] = \frac{A_{out}[3] * k_w * (\mathrm{T}[x][4][2] - \mathrm{T}[x][3][2]) * \Delta t}{\frac{w}{3}}$$

$$E_r[x][3][2] = A_{In}[3] * k_w * \frac{\mathrm{T}[x][2][2] - \mathrm{T}[x][3][2]}{\frac{\mathrm{w}}{3}} * \Delta \mathrm{t}$$

$$E_x[x][3][2](J) = A_x[3] * k_w * \frac{T[x+1][3][2] - 2 * T[x][3][2] + T[x-1][3][2]}{\Delta x} * \Delta t$$

$$E_\theta[x][3][2](J) = A_\theta[3] * k_w * \frac{T[x][3][1] - 2 * T[x][3][2] + T[x][3][3]}{\Delta x_\theta[3]} * \Delta t$$

Ring 4 final,

$$E_s[x][3][1] = \frac{A_{out}[3] * k_w * (\mathrm{T}[x][4][1] - \mathrm{T}[x][3][1]) * \Delta t}{\frac{w}{3}}$$

$$E_r[x][3][1] = A_{In}[3] * k_w * \frac{\mathrm{T}[x][2][1] - \mathrm{T}[x][3][1]}{\frac{\mathrm{w}}{3}} * \Delta \mathrm{t}$$

$$E_x[x][3][1](J) = A_x[3] * k_w * \frac{T[x+1][3][1] - 2 * T[x][3][1] + T[x-1][3][1]}{\Delta x} * \Delta t$$

$$E_\theta[x][3][1](J) = A_\theta[3] * k_w * \frac{T[x][3][4] - 2 * T[x][3][1] + T[x][3][2]}{\Delta x_\theta[3]} * \Delta t$$

Ring 3,

$$E_s[x][2][3] = \frac{A_{out}[2] * k_w * (\mathrm{T}[x][3][3] - \mathrm{T}[x][2][3]) * \Delta t}{\frac{w}{3}}$$

$$E_r[x][2][3] = A_{In}[2] * k_w * \frac{\mathrm{T}[x][1][3] - \mathrm{T}[x][2][3]}{\frac{\mathrm{w}}{3}} * \Delta \mathrm{t}$$

$$E_x[x][2][3](J) = A_x[2] * k_w * \frac{T[x+1][2][3] - 2 * T[x][2][3] + T[x-1][2][3]}{\Delta x} * \Delta t$$

$$E_\theta[x][2][3](J) = A_\theta[2] * k_w * \frac{T[x][2][4] - 2 * T[x][2][3] + T[x][2][2]}{\Delta x_\theta[2]} * \Delta t$$

$$A_{out}[2] = \left(\frac{\pi}{2}\left(r_0 - 2\frac{w}{3}\right) * \Delta x\right), A_{In}[2] = \left(\frac{\pi}{2}\left(r_0 - 3\frac{w}{3}\right) * \Delta x\right), A_x[2] = \left(\frac{\pi}{2} * \left(r_0 - 2\frac{w}{3} - \frac{w}{6}\right) * \frac{w}{3}\right),$$

$$A_\theta[2] = \left(\frac{w}{3} * \Delta x\right), \Delta x_\theta[2] = \frac{\pi}{2} * \left(r_0 - 2\frac{w}{3} - \frac{w}{6}\right)$$

Ring 2,

$$E_s[x][2][2] = \frac{A_{out}[2] * k_w * (\mathrm{T}[x][3][2] - \mathrm{T}[x][2][2]) * \Delta t}{\frac{w}{3}}$$

$$E_r[x][2][2] = A_{In}[2] * k_w * \frac{\mathrm{T}[x][1][2] - \mathrm{T}[x][2][2]}{\frac{\mathrm{w}}{3}} * \Delta\mathrm{t}$$

$$E_x[x][2][2](J) = A_x[2] * k_w * \frac{T[x+1][2][2] - 2 * T[x][2][2] + T[x-1][2][2]}{\Delta x} * \Delta t$$

$$E_\theta[x][2][2](J) = A_\theta[2] * k_w * \frac{T[x][2][3] - 2 * T[x][2][2] + T[x][2][1]}{\Delta x_\theta[2]} * \Delta t$$

Ring 1,

$$E_s[x][2][1] = \frac{A_{out}[2] * k_w * (\mathrm{T}[x][3][1] - \mathrm{T}[x][2][1]) * \Delta t}{\frac{w}{3}}$$

$$E_r[x][2][1] = A_{In}[2] * k_w * \frac{\mathrm{T}[x][1][1] - \mathrm{T}[x][2][1]}{\frac{\mathrm{w}}{3}} * \Delta\mathrm{t}$$

$$E_x[x][2][1](J) = A_x[2] * k_w * \frac{T[x+1][2][1] - 2 * T[x][2][1] + T[x-1][2][1]}{\Delta x} * \Delta t$$

$$E_\theta[x][2][1](J) = A_\theta[2] * k_w * \frac{T[x][2][4] - 2 * T[x][2][1] + T[x][2][2]}{\Delta x_\theta[2]} * \Delta t$$

Wax depo 3,

$$E_s[x][1][3] = \frac{A_{out}[x][1] * k_{w_{TopDepo}} * (\mathrm{T}[x][2][3] - \mathrm{T}[x][1][3]) * \Delta t}{w_{TopDepo}[x]}$$

$$E_x[x][1][3](J) = A_x[x][1] * k_{w_{TopDepo}} * \frac{T[x+1][1][3] - 2 * T[x][1][3] + T[x-1][1][3]}{\Delta x} * \Delta t$$

$$E_\theta[x][1][3](J) = A_\theta[x][1] * k_{w_{TopDepo}} * \frac{T[x][1][4] - 2 * T[x][1][3] + T[x][1][2]}{\Delta x_\theta[x][1]} * \Delta t$$

$$A_{out}[x][1] = \left(\frac{\pi}{2}\left(r_0 - 3\frac{w}{3}\right) * \Delta x\right), A_{In}[x][1] = \left(\frac{\pi}{2}\left(r_0 - 3\frac{w}{3} - w_{TopDepo}[x]\right) * \Delta x\right), A_x[x][1] = \left(\frac{\pi}{2} * \left(r_0 - 3\frac{w}{3} - \frac{w_{TopDepo}[x]}{2}\right) * w_{TopDepo}[x]\right),$$

$$A_\theta[x][1] = \left(w_{TopDepo}[x] * \Delta x\right), \Delta x_\theta[x][1] = \frac{\pi}{2} * \left(r_0 - 3\frac{w}{3} - \frac{w_{TopDepo}[x]}{2}\right)$$

For $E_r[x][1][3](J)$:

If `SlugFlow[xx]==1` (Slug flow):

$$E_r[x][1][3](J) = -A_{In}[x][1] * h_s[x] * \Delta t * (\bar{T}[x][1][3] - T_S[x]),$$

$$\bar{T}[x][1][3] = \frac{T[x+1][1][3] + T[x][1][3]}{2}$$

If `SlugFlow[xx]==0` (Not Slug flow):

$$E_r[x][1][3](J) = -\left(A_G[x][3] * h_G[x] * \Delta t * (\bar{T}[x][1][3] - T_G[x]) + A_L[x][3] * h_F[x] * \Delta t * (\bar{T}[x][1][3] - T_F[x])\right)$$

$$\bar{T}[x][1][3] = \frac{T[x+1][1][3] + T[x][1][3]}{2}$$

where

$$A_G[x][3] = \frac{\pi}{2}(r_i - w_{TopDepo}[x]) * \Delta x,\ A_L[x][3] = 0 \qquad if\ \phi^N < \frac{\pi}{2}$$

$$A_G[x][3] = \frac{\pi}{2}(r_i - w_{TopDepo}[x]) * \Delta x,\ A_L[x][3] = 0 \qquad if\ \frac{\pi}{2} \leq \phi^N \leq \frac{3*\pi}{2}$$

$$A_G[x][3] = \left((r_i - w_{TopDepo}[x]) * (2\pi - \theta^N) * \Delta x\right),\ A_L[x][3] = \left((r_i - w_{TopDepo}[x]) * \left(\theta^N - \frac{3\pi}{2}\right) * \Delta x\right) \qquad if\ \ \phi^N \geq \frac{3*\pi}{2}$$

Wax depo 2,

$$E_s[x][1][2] = \frac{A_{out}[x][1] * k_{w_{SideDepo}} * (\mathrm{T}[x][2][2] - \mathrm{T}[x][1][2]) * \Delta t}{w_{SideDepo}[x]}$$

$$E_x[x][1][2](J) = A_x[x][1] * k_{w_{SideDepo}} * \frac{T[x+1][1][2] - 2 * T[x][1][2] + T[x-1][1][2]}{\Delta x} * \Delta t$$

$$E_\theta[x][1][2](J) = A_\theta[x][1] * k_{w_{SideDepo}} * \frac{T[x][1][3] - 2 * T[x][1][2] + T[x][1][1]}{\Delta x_\theta[x][1]} * \Delta t$$

$$A_{out}[x][1] = \left(\frac{\pi}{2}\left(r_0 - 3\frac{w}{3}\right) * \Delta x\right), A_{In}[x][1] = \left(\frac{\pi}{2}\left(r_0 - 3\frac{w}{3} - w_{SideDepo}[x]\right) * \Delta x\right), A_x[x][1] = \left(\frac{\pi}{2} * \left(r_0 - 3\frac{w}{3} - \frac{w_{SideDepo}[x]}{2}\right) * w_{SideDepo}[x]\right),$$

$$A_\theta[x][1] = \left(w_{SideDepo}[x] * \Delta x\right), \Delta x_\theta[x][1] = \frac{\pi}{2} * \left(r_0 - 3\frac{w}{3} - \frac{w_{SideDepo}[x]}{2}\right)$$

For $E_r[x][1][2](J)$:

If `SlugFlow[xx]==1` (Slug flow):

$$E_r[x][1][2](J) = -A_{In}[x][1] * h_s[x] * \Delta t * (\bar{T}[x][1][2] - T_S[x]),$$

$$\bar{T}[x][1][2] = \frac{\bar{T}[x+1][1][2] + \bar{T}[x][1][2]}{2}$$

If `SlugFlow[xx]==0` (Not Slug flow):

$$E_r[x][1][2](J) = -\left(A_G[x][2] * h_G[x] * \Delta t * (\bar{T}[x][1][2] - T_G[x]) + A_L[x][2] * h_F[x] * \Delta t * (\bar{T}[x][1][2] - T_F[x])\right)$$

where

$$A_G[x][2] = \frac{\pi}{2}(r_i - w_{SideDepo}[x]) * \Delta x,\ A_L[2] = 0 \qquad if\ \phi^N < \frac{\pi}{2}$$

$$A_G[x][2] = \frac{(r_i - w_{SideDepo}[x])}{2}\left(\frac{3\pi}{2} - \theta^N\right) * \Delta x,\ A_L[x][2] = \frac{(r_i - w_{SideDepo}[x])}{2}\left(\theta^N - \frac{\pi}{2}\right) * \Delta x \quad if\ \frac{\pi}{2} \leq \phi^N \leq \frac{3*\pi}{2}$$

$$A_G[x][2] = 0,\ A_L[x][2] = \left((r_i - w_{SideDepo}[x]) * \frac{\pi}{2} * \Delta x\right) \qquad if\ \ \phi^N \geq \frac{3*\pi}{2}$$

Wax depo 1,

$$E_s[x][1][1] = \frac{A_{out}[x][1] * k_{w_{BotDepo}} * (\mathrm{T}[x][2][1] - \mathrm{T}[x][1][1]) * \Delta t}{w_{BotDepo}[x]}$$

$$E_x[x][1][1] = A_x[x][1] * k_{w_{BotDepo}} * \frac{T[x+1][1][1] - 2 * T[x][1][1] + T[x-1][1][1]}{\Delta x} * \Delta t$$

$$E_\theta[x][1][1] = A_\theta[x][1] * k_{w_{BotDepo}} * \frac{T[x][1][2] - 2 * T[x][1][1] + T[x][1][4]}{\Delta x_\theta[x][1]} * \Delta t$$

$$A_{out}[x][1] = \left(\frac{\pi}{2}\left(r_0 - 3\frac{w}{3}\right) * \Delta x\right), A_{In}[x][1] = \left(\frac{\pi}{2}\left(r_0 - 3\frac{w}{3} - w_{BotDepo}[x]\right) * \Delta x\right), A_x[x][1] = \left(\frac{\pi}{2} * \left(r_0 - 3\frac{w}{3} - \frac{w_{BotDepo}[x]}{2}\right) * w_{BotDepo}[x]\right),$$

$$A_\theta[x][1] = \left(w_{BotDepo}[x] * \Delta x\right), \Delta x_\theta[1] = \frac{\pi}{2} * \left(r_0 - 3\frac{w}{3} - \frac{w_{BotDepo}[x]}{2}\right)$$

For $E_r[x][1][1](J)$:

If `SlugFlow[xx]==1` (Slug flow):

$$E_r[x][1][1](J) = -A_{In}[x][1] * h_s[x] * \Delta t * (\bar{T}[x][1][1] - T_S[x]),$$

$$\bar{T}[x][1][1] = \frac{\bar{T}[x+1][1][1] + \bar{T}[x][1][1]}{2}$$

If `SlugFlow[xx]==0` (Not Slug flow):

$$E_r[x][1][1](J) = -\left(A_G[x][1] * h_G[x] * \Delta t * (\bar{T}[x][1][1] - T_G[x]) + A_L[x][1] * h_F[x] * \Delta t * (\bar{T}[x][1][1] - T_F[x])\right)$$

where

$$A_G[x][1] = (r_i - w_{BotDepo}[x])\left(\frac{\pi}{2} - \theta^N\right) * \Delta x,\ A_L[x][1] = r_i * \theta^N \qquad if\ \phi^N < \frac{\pi}{2}$$

$$A_G[x][1] = 0,\ A_L[x][1] = \left((r_i - w_{BotDepo}[x]) * \frac{\pi}{2} * \Delta x\right) \qquad if\ \frac{\pi}{2} \le\ \phi^N \le \frac{3*\pi}{2}$$

$$A_G[x][1] = 0,\ A_L[x][1] = \left((r_i - w_{SideDepo}[x]) * \frac{\pi}{2} * \Delta x\right) \qquad if\ \phi^N \ge \frac{3*\pi}{2}$$

Now, temperature increase due for each wall segment can be calculated as follows:

$$T^{t+1}[x][WL][RS] = T^t[x][WL][RS] + \frac{E_s[x][WL][RS] + E_r[x][WL][RS] + E_x[x][WL][RS] + E_\theta[x][WL][RS]}{A_x[RS]\Delta x \rho_w C_{p_w}}$$

and for the deposit sections, the following relation can be used as follows:

$$T^{t+1}[x][1][RS] = T^t[x][1][RS] + \frac{E_s[x][1][RS] + E_r[x][1][RS] + E_x[x][1][RS] + E_\theta[x][1][RS]}{A_x[x][RS]\Delta x \rho_{Depo} C_{Depo}}$$

For the next step, the fluids' temperatures are calculated from the following relations:

The energy transferred from the wall to the liquid is expressed by:

$$E_{wf}[x] = \sum_{RS=1}^{4} A_L[x][RS] * h_L[x] * \Delta t * \left(\frac{T^t[x+1][4][\mathrm{RS}] + T^t[x][4][\mathrm{RS}]}{2} - T_F^t[x]\right)$$

and the transferred heat from the shed liquid is considered as

$$E_{cf}[x] = \left((v_{Tb} - v_{LTB}[x+1]) * A_{p_{ef}}[x+1] * H_{LTB}[x+] * \rho_L * Cp_L * \Delta t * T_F^t[x+1]\right)_{x+1} - \left((v_{Tb} - v_{LTB}[x]) * A_{p_{ef}}[x] * H_{LTB}[x] * \rho_L * Cp_L * \Delta t * T_F^t[x]\right)_x$$

$$T_F^{t+1}[x] = T_F^t[x] + \frac{E_{wf}[x] + E_{cf}[x]}{\left(H_{LTB}[x] A_{p_{ef}} * \Delta x * \rho_L * Cp_L\right)_x}$$

Similarly, for gas phase we have:

$$E_{wg}[x] = \sum_{RS=1}^{4} A_G[x][RS] * h_g[x] * \Delta t * \left(\frac{T^t[x+1][4][RS] + T^t[x][4][RS]}{2} - T_G^t[x]\right)$$

and

$$E_{cg}[x] = cv_s(1 - H_{LLS})\left[\left(A_{p_{ef}}[x+1]Cp_G\rho_G T_G[x+1]\right)_{x+1} - \left(A_{p_{ef}}[x]Cp_G\rho_G T_G[x+1]\right)_x\right]\Delta t$$

$$T_G^{t+1}[x] = T_G^t[x] + \frac{E_{wg}[x] + E_{cg}[x]}{\left(\left[(1 - H_{LTB}[x])A_{p_{ef}}[x]\Delta x\right] * (Cp_G\rho_G)\right)_x}$$

and for the slug section:

$$E_{ws}[x] = \left(2\pi(r_i - \overline{w}_{depo}[x])\Delta x\right)h_s[x]\Delta t\left[\frac{\sum_{RS=1}^{4} T^t[x+1][4][RS] + T^t[x][4][RS]}{8} - T_S[x]\right]$$

$$E_{cs}[x] = cA_{p_{ef}}[x]v_m[(\rho_s Cp_s T_s[x+1])_{x+1} - (\rho_s Cp_s T_s[x])_x]$$

$$T_S^{t+1}[x] = T_S^t[x] + \frac{E_{ws}[x] + E_{cs}[x]}{A_{p_{ef}}[x]\Delta x * \rho_s Cp_s}$$

The above formulation is for the case where wax deposition is present. However, in order to verify our heat transfer modeling, we needed to analyze our model for the case of no deposition and constant heat flow. The purpose is to obtain a time-averaged convective heat transfer coefficient for slug flow and then to compare it to correlations available in literature. From the following derivation, we calculated the average heat transfer coefficient of the slug flow from the developed heat transfer model for the case of constant heat flux and no deposition.

$$Q_{tot}\left[\frac{J}{m.s}\right] = S[m] * h_{TP}\left[\frac{J}{m^2.s.°K}\right] * (T - T_W)[°K]$$

$$\overline{h_{TP}} = \frac{\int_0^{t_u}\frac{(Q_{tot})}{S}\frac{dt}{t_u}}{\int_0^{t_u}(T - T_W)\frac{dt}{t_u}}$$

$$Q_{tot} = Q_s + Q_f$$

$$\overline{h_{TP}} = \frac{\int_0^{t_s}\frac{Q_s}{\pi D}\frac{dt}{t_u} + \int_{t_s}^{t_u}\frac{Q_f}{\pi D}\frac{dt}{t_u}}{\int_0^{t_s}(T_s - T_{Ws})\frac{dt}{t_u} + \int_{t_s}^{t_u}(T_f - T_{Wf})\frac{dt}{t_u}}$$

I will use the above equation for calculation of average convective heart transfer coefficient of slug flow. However, I needed to make a little bit of adjustment to the above equation based on what is reported in my program.

$$V_{TB} = \frac{d_x}{d_t} => d_t = \frac{d_x}{V_{TB}}$$

So,

$$\overline{h_{TP}} = \frac{\int_0^{t_s} \frac{Q_s}{\pi D}\frac{dt}{t_u} + \int_{t_s}^{t_u} \frac{Q_f}{\pi D}\frac{dt}{t_u}}{\int_0^{t_s}(T_s - T_{Ws})\frac{dt}{t_u} + \int_{t_s}^{t_u}\left(T_f - T_{Wf}\right)\frac{dt}{t_u}}$$

$$\overline{h_{TP}} = \frac{\int_0^{L_s} \frac{Q_s}{\pi D}dx + \int_{L_s}^{L_u} \frac{Q_f}{\pi D}dx}{\int_0^{L_s}(T_s - T_{Ws})dx + \int_{L_s}^{L_u}\left(T_f - T_{Wf}\right)dx}$$

Where,

$$Q_s\left[\frac{J}{m.s}\right] = \frac{E_{ws}[J]}{\Delta_x[m] * \Delta_t[s]}$$

$$Q_f\left[\frac{J}{m.s}\right] = \frac{E_{wf}[J] + E_{wG}[J]}{\Delta_x[m] * \Delta_t[s]vr}$$

In the literature, there are correlations that approximates the ratio of slug flow Nusselt number and single-phase flow Nusselt number. From Dong and Hibiki (2018), two correlations were utilized as follow:

Correlation 1:

$$\frac{Nu_{2\phi}}{Nu_{1\phi}} = (1-\alpha)^{1.28}\Phi_f^2$$

where Φ_f^2 is the two-phase multiplier and can be calculated as:

$$\Phi_f^2 = \frac{1}{(1-\alpha)^m}$$

And m is usually between 1.75 and 2.0.

Correlation 2:

$$\frac{Nu_{2\phi}}{Nu_{1\phi}} = (1-\alpha)^{-0.194}(1 + 0.687X^{-0.7})$$

Where X is the Lockhart-Martinelli parameter and can be approximated by:

$$X = \sqrt{\frac{\left(\frac{dp}{dz}\right)_{F,f}}{\left(\frac{dp}{dz}\right)_{F,g}}}$$

For both correlations, the following Nusselt number correlation was proposed:

$$Nu_{1,\phi} = \frac{\left(\frac{f}{8}\right)\left(Re_f - 1000\right)pr_f}{1 + 12.7\sqrt{\frac{f}{8}}\left(pr_f^{\frac{2}{3}} - 1\right)}\left[1 + \left(\frac{D}{L}\right)^{\frac{2}{3}}\right]$$

From the following graph,

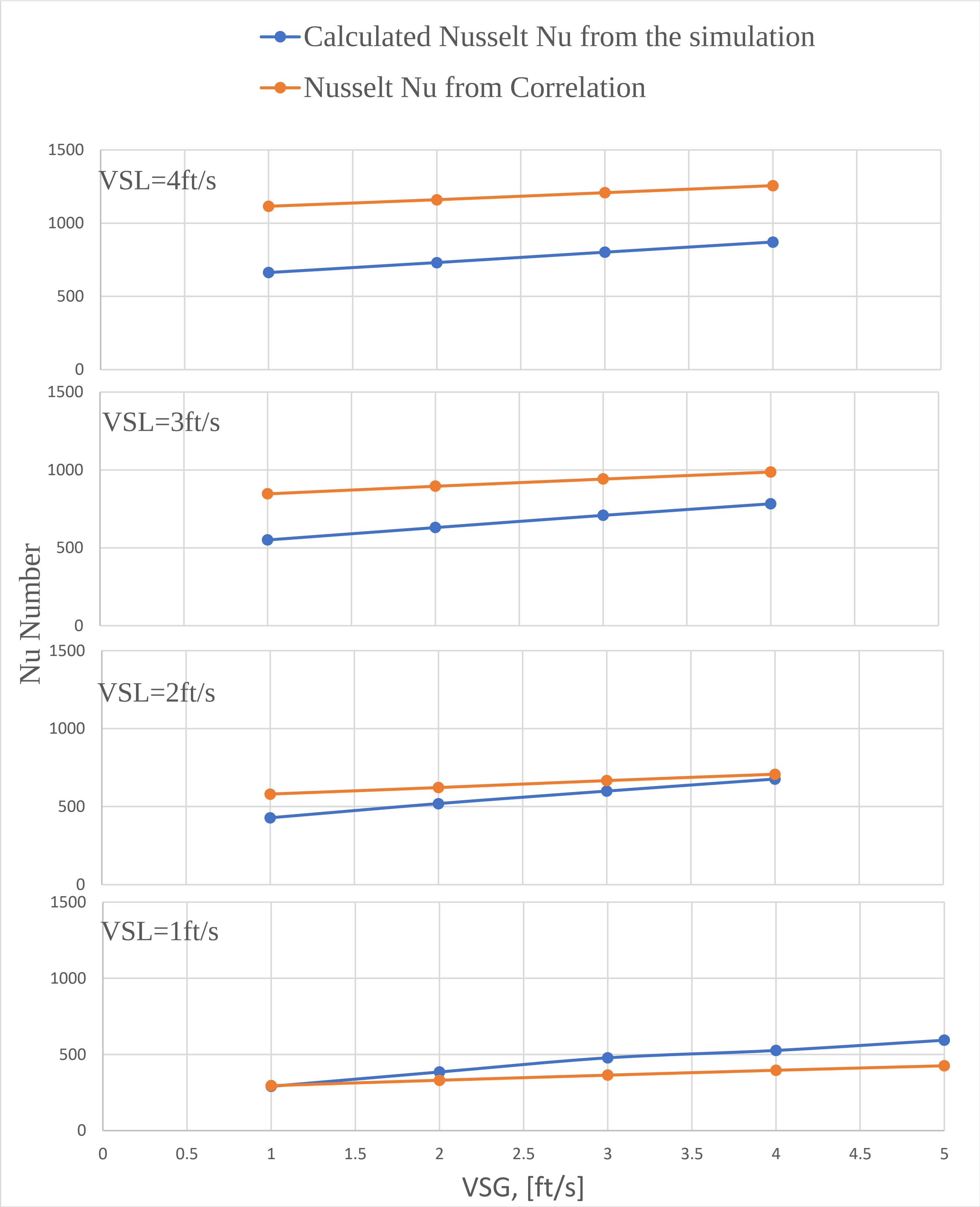

Figure 12: Nusselt number comparison between Dong and Hibiki correlation and the developed heat transfer mode

Implementation details:

One important aspect of the model is to correctly choose the time step and axial intervals. Therefore, it will be known which axial block contains either slug or film. This is very important because, formulas are different for slug and film sections.

Please consider the following schematic:

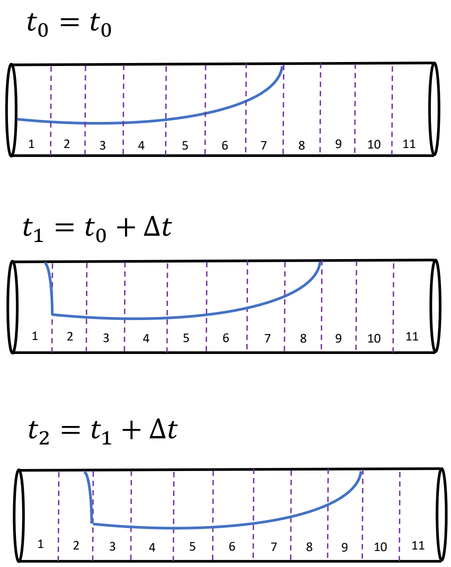

The above discretization and time step determination make it possible to know the status of each grid block at a certain time (slug or film). Interestingly, the number of grid blocks which are assigned to film and to slug are constant. In the developed code, a Boolean array (SlugFlow) has been defined to tell if a grid block is slug or it is film at different times.

The SlugFlow values for a case of N=22 is shown for example purposes as:

t0	0	0	0	0	0	0	0	0	0	0	0	0	0	0	0	0	0	0	0	1	1	1
t1	1	0	0	0	0	0	0	0	0	0	0	0	0	0	0	0	0	0	0	0	1	1
t2	1	1	0	0	0	0	0	0	0	0	0	0	0	0	0	0	0	0	0	0	0	1
t3	1	1	1	0	0	0	0	0	0	0	0	0	0	0	0	0	0	0	0	0	0	0
t4	0	1	1	1	0	0	0	0	0	0	0	0	0	0	0	0	0	0	0	0	0	0
t5	0	0	1	1	1	0	0	0	0	0	0	0	0	0	0	0	0	0	0	0	0	0
t6	0	0	0	1	1	1	0	0	0	0	0	0	0	0	0	0	0	0	0	0	0	0
t7	0	0	0	0	1	1	1	0	0	0	0	0	0	0	0	0	0	0	0	0	0	0

t8	0	0	0	0	0	1	1	1	0	0	0	0	0	0	0	0	0	0	0	0	0	0
t9	0	0	0	0	0	0	1	1	1	0	0	0	0	0	0	0	0	0	0	0	0	0

The zero grid blocks contain film while blue ones contain slug

[1] Y. Taitel and D. Barnea, Two-phase slug flow. Advances in heat transfer. 1990, http://www.sciencedirect.com/science/article/pii/S0065271708700261.

[2] H. Zhang, Q. Wang, C. Sarica, and J. Brill, Unified model for gas-liquid pipe flow via slug dynamics-part 1: Model development. Journal of energy resources technology. 2003, 125 (4): 266–273 goo.gl/sQopJ2.

[3] G. Gregory, M. Nicholson, and K. Aziz, Correlation of the liquid volume fraction in the slug for horizontal gas-liquid slug flow. International Journal of Multiphase. 1978, http://www.sciencedirect.com/science/article/pii/030193227890023X.

[4] O. Shoham, Mechanistic modeling of gas-liquid two-phase flow in pipes. 2006, .

[5] T. Niu, Heat transfer during gas-liquid slug flow in horizontal tubes. 1976, .